# Multi-scale transport dynamics dominated by multiple dissipation mechanisms near the critical gradient

Y. Kishimoto 1), K. Miki 1*), J.Q. Li 1), N. Miyato 2), Z.X. Wang 1), J. Anderson 3)


1) Graduate School of Energy Science, Kyoto University, Uji, Kyoto 611-0011, Japan,

2) Japan Atomic Energy Agency, Naka, Ibaraki-ken 311-0193, Japan

3) Department of Applied Mathematics, University of Sheffield, S3 7RH, UK

   * Present address: University of California, San Diego, La Jolla, California, USA


E-mail contact of main author:    kishimoto@energy.kyoto-u.ac.jp

**Abstract:** A new class of transient transport near the critical gradient (CG) referred to as *GAM growing intermittency* due to the collision-less GAM damping has been found based on Landau-fluid simulation[*Miki, et al., Phys. Rev. Letts. 99, 145003 (2007)*]. Here, we present a new predator-prey model to understand the essential features of the growing intermittency. We have also extended the simulation model by taking into account the collisional zonal flow (ZF) damping. Due to the mixture of two kinds of damping mechanisms, i.e. the GAM damping and collisional damping, the growing intermittency is found to recursively appear accompanied with complex envelope modulation to ZFs over collisional (or transport) time scale. Furthermore, we have investigated the effect of *zonal pressure* (ZP) near the CG, which also works as a dissipation mechanism. The multiple dissipation mechanisms are found to synergetically couple each other and lead plasmas to complex dynamical transport over long time scale.

## 1   Introduction

Transport near the critical gradient (CG) where the multiple states dominated by different physical processes coexist is especially important since the plasma has to inevitably cross such a region in reaching high pressure states. Nonlinearly generated large scale structures such as zonal flows (ZFs) and geodesic acoustic modes(GAMs) play an important role in regulating the transport near the CG[1]. Nonlinear up-shift of the CG, namely, the Dimits shift[2], is a typical example. An intermittent dynamics has been observed near the critical gradient due to collisional damping of ZFs in ion temperature gradient (ITG) driven turbulence[3]. Recently, the GAM, which is an oscillatory counterpart of the ZF in toroidal plasmas coupled with pressure perturbation of $(m,n)=(1,0)$, has been extensively studied, since it significantly changes the characteristics of ZFs and then the transport[4-9], where $m$ and $n$ denote poloidal and toroidal wave number, respectively. We have studied the effect of GAMs on the CG phenomena based on the global toroidal Landau-fluid simulations [9] by choosing the temperature gradient, i.e. $R/L_{Ti}$, slightly above the linear instability threshold [10]. A prominent intermittent state associated with GAMs near the CG region has been found as shown in Fig.1(a). This new intermittency is referred to as *GAM growing intermittency*,

which is qualitatively different from those originated from the collisional damping [3]. In this work, we propose a four-field model to understand the complex GAM dynamics and analyze the characteristics of the GAM growing intermittency in the CG regime. Furthermore, we extend the simulation by including not only the GAM damping, but also the collisional ZF damping and small scale pressure modulation, i.e. so called ZP effect, to investigate the turbulent transport in collisional time scale regulated by multiple dissipation mechanisms.

## 2 An extended predator-prey model for GAM growing intermittency

### 2.1 Minimal four-field predator-prey model

Here, we present a theoretical model to analyze the underlying physical processes in the GAM growing intermittency. In the framework of the fluid model [9], keeping the total energy conservation in mind, we can derive an equation system of GAM dynamics with respect to the ZF $\langle \upsilon_E \rangle$, the GAM $\langle p \sin\theta \rangle \equiv p_{10}$ and anisotropic ion sound velocity $\langle \upsilon_\parallel \cos\theta \rangle \equiv \upsilon_{10}$. By using following normalization and definition of the variables $(t;U;G;V) \rightarrow \left( t / \sqrt{T_{eq}} ; \langle \upsilon_E \rangle ; \langle p \sin\theta \rangle / \sqrt{T_{eq}} \, p_{eq} ; \langle \upsilon_\parallel \cos\theta \rangle \right)$, we can obtain

$$\partial_t U = -\beta G + \widehat{N}_{[\phi,\phi]} \quad , \tag{1}$$

$$\partial_t G = \beta' U - \gamma_{LD} G + \beta_2 V + \widehat{N}_{[\phi,p]} \quad , \tag{2}$$

$$\partial_t V = -\beta_2' G + \widehat{N}_{[\phi,\upsilon_\parallel]} \quad , \tag{3}$$

where $N \equiv E_{turb.}$, $U \equiv \langle \upsilon_E \rangle$, $G \equiv \sqrt{3/4} \langle p \sin\theta \rangle$, $V \equiv \sqrt{2} \langle \upsilon_\parallel \cos\theta \rangle$. $\beta = 2\varepsilon$, $\beta' = \varepsilon(\Gamma + \tau)$, $\beta_2 = ((\Gamma + \tau)\varepsilon/q$, $\beta_2' = \varepsilon/q$ with $\varepsilon = a/R$, and the Landau damping rate is given by $\gamma_{LD} = T_{eq}\sqrt{8/\pi} \, \varepsilon/q$. The nonlinear terms are given by $\widehat{N}_{[\phi,\phi]} = -\langle \widetilde{\upsilon}_{E_r} \widetilde{\Omega} \rangle$, $\widehat{N}_{[\phi,p]} = -\langle [\widetilde{\phi}, \widetilde{p}] \sin\theta \rangle / p_{eq}$, and $\widehat{N}_{[\phi,\upsilon_\parallel]} = -\langle [\widetilde{\phi}, \widetilde{\upsilon}_\parallel] \cos\theta \rangle$. $T_{eq}=1$ is assumed for simplicity. Starting from Eqs.(1)-(3), the GAM oscillation can be analyzed by neglecting the nonlinear terms, i.e.,

$$\partial_t^2 G + \gamma_{LD} \partial_t G + \omega_G^2 = 0 \quad , \tag{4}$$

with $\omega_G = \sqrt{\omega_{GAM}^2 + \omega_{sound}^2} = \sqrt{\beta\beta' + \beta_2\beta_2'}$. Note that the nonlinear terms work as the sources to trigger the GAM dynamics. Instead of these nonlinear terms, here we simply assume the
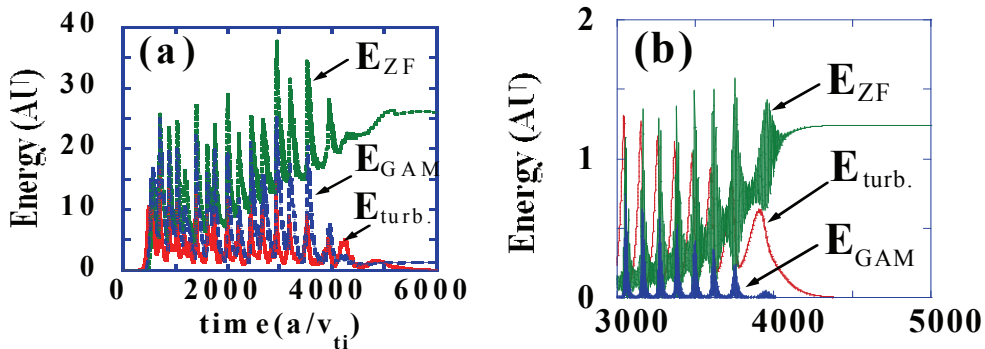


*Fig.1 Time evolution of turbulence ($E_{turb.}$), ZF ($E_{ZF}$), and GAM($E_{GAM}$) energy for (a) nonlinear simulation in the case of $R/L_T$=4.05 and $q_0$=2.1 [Ref.10] and (b) corresponding four- field model, Eqs.(8)-(11), in the case of $\gamma_L$=0.05.*

source effect as initial value problem $(U_0, G_0, V_0)_{t=0}$. Then Eq.(4) is solved as follows;

$$U = A_U \exp(-\gamma_{LD}t/2)\sin(\omega_r t + \delta_1) + C_U \qquad , \qquad (5)$$

$$G = A_G \exp(-\gamma_{LD}t/2)\sin(\omega_r t + \delta_2) \qquad , \qquad (6)$$

$$V = A_V \exp(-\gamma_{LD}t/2)\sin(\omega_r t + \delta_1) + C_V \qquad , \qquad (7)$$

where $\omega_r = \sqrt{\omega_G^2 - (\gamma_{LD}/2)^2}$, and $(A_U, A_G, A_V)$ and $(C_U, C_V)$ are constants determined by the initial conditions. Here, $C_U$ and $C_V$ are expressed $C_U = (U_0 - 2qV_0)/(1 + 2q^2)$ and $C_V = -qC_U$. $\delta_1$ and $\delta_2$ are the phase factors also determined by initial conditions and $\Delta\delta \equiv \delta_1 - \delta_2 \approx \pi/2$ is estimated. As seen in equations (5)-(7), each variable exhibits the damping oscillation ascribed from the GAM oscillation and decay due to the Landau damping. It is noticed that the undamped residual part can be survived in $U$ and $V$ as a stationary ZF and ion parallel velocity after the complete damping of $G$, which balances in accordance with $\beta'C_U + \beta_2 C_V = 0$. Hence, it is expected that the residual part of the ZFs accumulates during the repetition of the burst and gradually increase as seen in Fig.1(a).

To understand the physical processes in intermittent dynamics in a self-consistent manner, we construct a four-field equation system as a predator-prey model based on Eqs.(1)-(3) with the turbulence evolution. By defining the turbulent energy as $N = \sum |\tilde{\phi}_{(m,n)}|^2$, we have :

$$\partial_t N = \gamma_L N - \gamma_{NL} N^2 - \alpha_1 U^2 N - \alpha_2 G^2 N - \alpha_3 V^2 N \qquad , \qquad (8)$$

$$\partial_t U = \tfrac{1}{2}\alpha_1 UN - \omega_{GAM} G - \tfrac{1}{2}\gamma_{damp} U \quad , \qquad (9)$$

$$\partial_t G = \tfrac{1}{2}\alpha_2 GN + \omega_{GAM} U + \omega_{sound} V - \gamma_{LD} G \qquad , \qquad (10)$$

$$\partial_t V = \tfrac{1}{2}\alpha_3 VN - \omega_{sound} G \qquad , \qquad (11)$$

where $\gamma_L$ and $\gamma_{NL}$ are the linear growth rate and the nonlinear damping rate, respectively. $\gamma_{damp}$ is the collisional damping rate of the ZFs. Note here that contrary to the conventional predator-prey model[1,11] where the ZFs are expressed in the unit of energy, e.g. $U^2$, Eqs. (9)-(11) are described not in terms of $U^2$, $G^2$, and $V^2$, but in terms of $U$, $G$ and $V$, in order to represent the oscillatory characteristics of the GAM and ion parallel sound wave. $(\alpha_1, \alpha_2, \alpha_3)$ represent the strength of nonlinear coupling including the cross-coupling [12] among the ZFs, GAMs and sound waves as well as the directions of energy flow from turbulence $N$ to the ZF $U$, the GAMs $G$, and the sound wave $V$, respectively. In this minimal model, it is assumed that the nonlinear cross-coupling, i.e., the off-diagonal terms in equations (9)-(11) have been effectively absorbed in the diagonal terms for simplicity. The collision effect on the ZFs is neglected here to manifest the effect of GAM damping. Note that this model satisfies the total energy conservation in the absence of linear driving source and damping terms.

## 2.2   Numerical analysis of four-field equation system

In analyzing the predator-prey model, we employ the parameters as the following, $\gamma_L$=0.05, $\gamma_{NL}$=0.003, $\gamma_{damp}$=0, and $q$=2.1, which roughly follow those used in the simulation of

Fig.1(a). Note that different GAM features depend on the relative magnitude between $\alpha_1$, $\alpha_2$ and $\alpha_3$, which characterizes the nonlinear energy flow from $N$ to $(U,\ G,\ V)$, the following three cases are analyzed.

*Case 1* ($\alpha_1 < \alpha_2$): Here, we choose $\alpha_1 = 0.05$, $\alpha_2 = 0.5$ and $\alpha_3 = 10^{-4}$, respectively. This case physically corresponds to that the Reynolds stress is less dominant than the nonlinear coupling term between turbulence and the GAMs. The time evolution of ($N,\ U,\ G$) as shown in Fig.1(b) can well reproduce the basic features of the GAM intermittency such as the quasi-period bursts, gradual increase of the ZFs and turbulence quenching observed in Fig.1(a). The accumulation of undamped residue of the ZFs is confirmed. Fig.2 shows the details for the specific time interval of a burst in Fig.1(b). As turbulence energy $N$ reaches a critical value that satisfies the relation $\gamma_L - \gamma_{NL} N \cong E_\alpha (\equiv \alpha_1 E_U + \alpha_2 E_G + \alpha_3 E_V)$, the abrupt growth of $E_U$, $E_G$, and $E_V$ and successive damping accompanied with typical GAM oscillation are observed as seen in Fig. 2(b). The turbulence also suffers damping once the relation $\gamma_L - \gamma_{NL} N < E_\alpha$ is satisfied at $t \cong 1190$ as seen in Fig.2(a). Followed by the turbulence, the GAM damping starts after the relation $\gamma_{LD} > \alpha_2 N/2$ is satisfied as seen in Fig.2(c). The characteristics of the abrupt growth of $G$ are investigated by solving Eq.(10) under the condition $\beta' U + \beta_2 V = 0$. Here it is assumed that $U$ and $V$ are almost balanced, and $N = N_0 \exp(\gamma_L t)$ is satisfied where $N_0$ is a reference amplitude when $\partial_t G = 0$, i.e. $\gamma_{LD} = \alpha_2 N_0 / 2$ is fulfilled. The solution is approximately given by

$$G = G_0 \exp\left[(\gamma_{LD}/\gamma_L)e^{\gamma_L t} - \gamma_{LD} t\right] \cong G_0 \exp(\gamma_L \gamma_{LD} t^2 / 2)\ ,\qquad (12)$$

showing faster growth than the linear instability. The time scale of the abrupt growth is evaluated as $\tau_b \sim \sqrt{2/\gamma_L \gamma_{LD}}$. In the present parameters, $\tau_b \sim 17.5$ is measured, which is consistent with that observed in Fig.2. It is noted that the typical damping rate of $N$ is characterized by $E_\alpha$ after the condition $\gamma_N - \gamma_{NL} N < E_\alpha$ is satisfied. The damping of $N$ is ceased when $E_\alpha$ crosses again $\gamma_L - \gamma_{NL} N$ as seen in Fig.2(b) at $t\sim 1212$, and then $N$ once more starts to grow linearly. During the phase of Landau damping, $E_G$ is quenched while a certain equilibrium levels of $E_U$ and $E_V$ are sustained, which are described as $C_U$ and $C_V$, respectively. This process leads to the accumulation of the ZFs as shown in Fig.1(a).
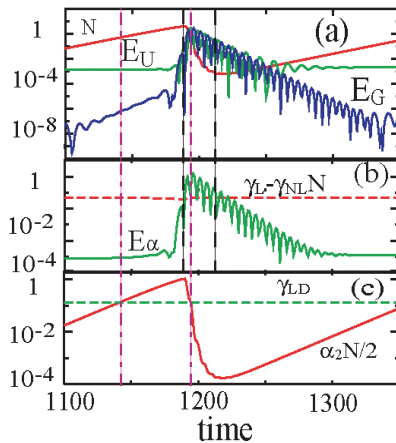


*Fig. 2 (a) Time evolution of N, $E_U$, and $E_G$ for the case of the extended minimum model for the time interval of one burst (1100<t <1250).*
*(b): Temporal evolution of ($\gamma_L$-$\gamma_{NL}N$) and $E_a$.*
*(c): Temporal evolution of $\alpha_2N/2$ and $\gamma_{LD}$.*
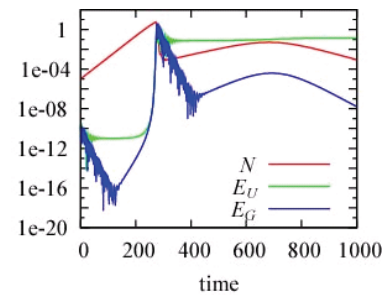


*Fig. 3   Time evolution of N, $E_U$ and $E_G$ in case of $\alpha_1$ is dominant (case 2).*

*Case 2* ($\alpha_1 > \alpha_2$): Contrary to the *case 1*, here we choose $\alpha_1 = 0.5$, $\alpha_2 = 0.05$, and $\alpha_3 = 10^{-4}$, respectively. The result is shown in Fig.3. In this case, the Reynolds stress is dominant compared with the nonlinear coupling between turbulence and the GAMs. As seen in Fig.3, after the single burst of the turbulence occurs, the residual ZF immediately quenches both turbulence and the GAMs and causes the decoupling of the ZFs and the GAMs. This may correspond to the single burst nature observed in the fluid simulation [10], in which the turbulence is completely suppressed by the ZFs. As we see in *cases 1* and *2*, when $\alpha_2 > \alpha_1$ is satisfied, multiple bursts are exhibited successively, whereas the dynamics is dominated by the single burst when $\alpha_1 > \alpha_2$. The change of the dynamics between *case 1* and *case 2* takes place at $\alpha_1 \approx \alpha_2$. This suggests that a certain amount of energy flow directly from turbulence to $p_{10}$ pressure perturbation may be necessary to have the growing intermittency as seen in Fig.1(b). The physical mechanism for what the relative relation between $\alpha_1$ and $\alpha_2$ provides different dynamical features may be understood as follows. The turbulence saturation takes place when the suppression term $-E_\alpha \cong -(\alpha_1 E_U + \alpha_2 E_G + \alpha_3 E_V)$ overwhelms the linear driving term $\gamma_L$ in equation (8) in both *case 1* and *case 2*. Namely, both $\alpha_1$ and $\alpha_2$ (and/or $\alpha_1 E_U$ and $\alpha_2 E_G$) decide the saturation level of turbulence $N$ as a whole. On the other hand, the contribution of the GAMs to $E_\alpha$, i.e. the term $\alpha_2 E_G$, inevitably suffer the collisionless damping even after the saturation. Due to this reason, the turbulence grows again after the quench in *Case 1* ($\alpha_1 < \alpha_2$) leading to a multiple-burst since $\alpha_2 E_G$ is damped. On the other hand, in *Case 2* ($\alpha_1 > \alpha_2$), turbulence is suppressed mainly by the undamped ZFs, i.e. $\alpha_1 E_U$, which does not suffer damping. Namely, in *Case 2*, once the quench of turbulence takes place, next burst does not happen. This feature is consistent with the analysis based on Eqs.(5)-(7) that the residual components $C_U$ and $C_V$ do not depend on the initial condition $G_0$ which is equivalent to the energy inflow from turbulence to $p_{10}$ pressure perturbation through nonlinear coupling. This supports the observation that $\alpha_2$ does not contribute the accumulation of undamped residues. Thus, it is found that the relative relation between $\alpha_1$ and $\alpha_2$ determine "the quality of saturation" and subsequent dynamics.
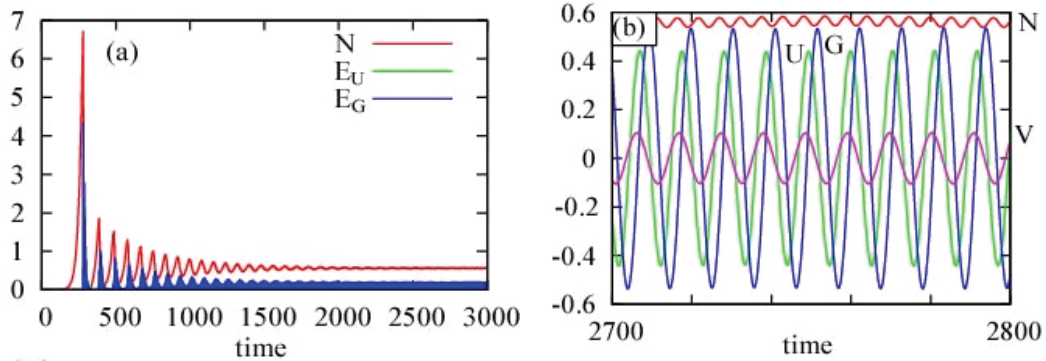


Fig. 4 (a) Time evolution of N, $E_U$ and $E_G$ during the time 0<t<3000 in case 3, (b) Time evolution of N. U. G. and V during the time 2700<t<2800.

*Case 3*: This case corresponds to the *Case 1* for $\alpha_1$ and $\alpha_2$, but a negative value $\alpha_3 = -0.05$ is chosen. In this case, the turbulence is not completely quenched, but approaches to a steady state level gradually as shown in Fig.4(a). The other components such as *U, G,* and *V* show an oscillatory feature which corresponds to GAM oscillation. It is found that the phase shift between *U* and *V* is almost the same and that between *U* and *G* shows a difference nearly by $\pi/2$, which is consistent with the analytical result obtained in equations (8)-(10). Enough energy backflow from ion parallel sound velocity to the turbulence can sustain the steady state level against the suppression effect of the ZFs.

## 3    Simulations with multiple dissipations

Turbulent transport is closely related to the dynamics of the ZFs and GAMs, which depend on the dissipation mechanisms. In the preceding section, we only discussed the collisionless damping of the ZFs due to the GAM dynamics in the growing intermittency. In principle, any dissipations for the ZFs, such as the static collision damping [3] or the dynamic GAM dampling [10] or multi-scale turbulence interaction[13], may alter the transport characteristics. Here we extend the simulation to involve the collisional damping of the ZFs and also the effects of the ZP in the CG regime.

### 3.1    Mixed dissipations with collision and GAM damping

The collisional damping is important for ZF dynamics in real plasmas, which can also cause turbulent transport intermittency [3]. Here we perform simulations including collisional effect on the ZFs by changing the *viscosity* for ZFs while the ZFs are damped through the GAM dynamics. Other parameters are the same as those in Fig.1(a). In the moderate viscosity case $D = 10^{-3}$ as shown in Fig.5(a), after the first growing intermittency, the stationary ZF is damped due to the collision and then the second intermittent cycle is triggered. The second one exhibits a complex feature where the accumulation of un-damped stationary ZF competes
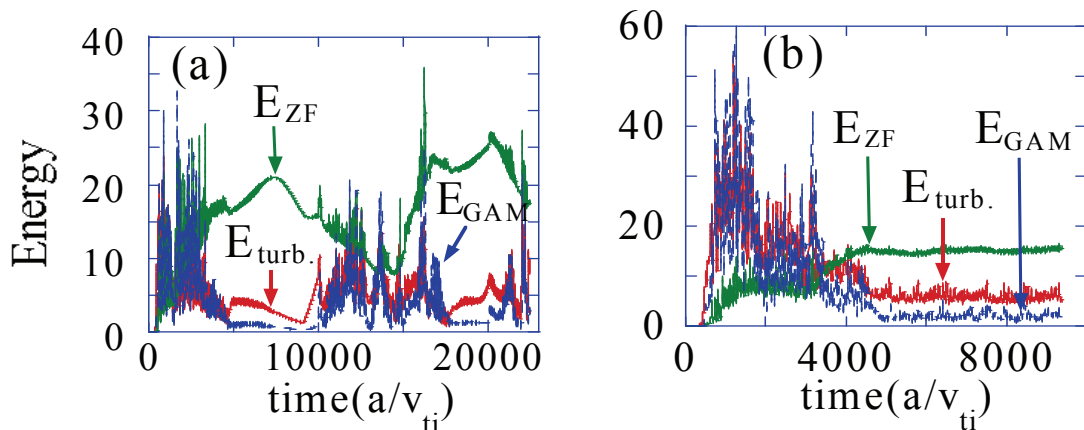


Fig.5    Time evolution of $E_{turb}$, $E_{ZF}$, and $E_{GAM}$ for (a) $D=10^{-3}$ and (b) $D=10^{-2}$.

with the collisional damping, leading to a long time scale envelope modulation to ZFs with irregular period. For larger viscosity $D = 10^{-2}$ [Fig.5(b)], ZFs stay in a low level so that clear growing intermittency does not appear. Instead, a new type of oscillation where the turbulence directly couples with the anisotropic pressure perturbation can be seen in $t \leq 4000$. Similar characteristics have been discussed in experiments [8]. As the viscosity increases, the ZFs become weak due to the collision effect so that the ZF residual part becomes lower. The saturation level of the GAMs increases with the collision effect. The turbulence energy becomes higher due to the reduction of stationary ZFs. Note that the collisional damping provides another time scale to GAM intermittency system. Interestingly, two different types of intermittency due to both the GAM dynamics and the collisional damping appear separately when the time scale of the latter is much different from that of GAM damping as seen in Fig.5. Otherwise, the intermittent dynamics is almost diminished due to interference and a steady state is found to be generated where turbulence, ZFs and the GAMs coexist.

### 3.2   Mixed dissipations with zonal pressure and GAM damping

Zonal pressure is a nonlinearly generated secondary fluctuation like the ZF. It can modify the equilibrium pressure profile so that it may provide one kind of saturation mechanisms of the turbulence. Meanwhile, the ZP couples with the GAM through the toroidal coupling so that it may be involved in the GAM growing intermittency in the CG regime. Here we perform another simulation ZPs but without collisional damping based on the simulation in Fig.1(a). In the plasma dominated by the GAMs, the ZP is influenced by the GAM oscillation through the toroidal coupling, so that it also reveals oscillatory nature as shown by the radial dependence of temperature scale length in Fig.6(a). Once the pressure profile locally crosses the CG due to the ZPs, probabilistically, the turbulence is reduced so that the decoupling between ZFs and GAMs happens. As a result, the growing intermittency is suddenly terminated as shown in Fig.6(b).
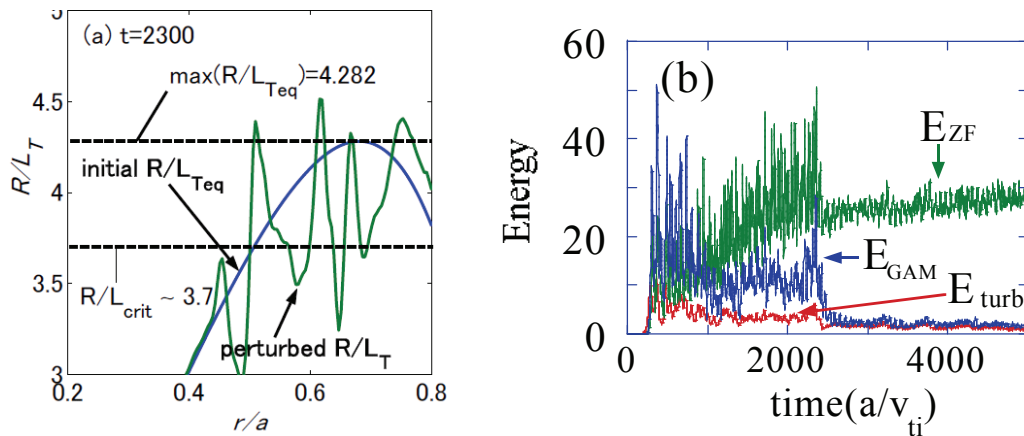


*Fig.6 (a) Radial dependence of $R/L_T$ for initial temperature profile and that for t=2300. (b) Time evolution of $E_{turb}$, $E_{ZF}$, and $E_{GAM}$ with the ZP effect.*

## 4   Summary and conclusion

We have proposed a four-field minimum model to describe the growing intermittency of turbulence associated with the GAM observed in our toroidal Landau-fluid simulations[10]. The different nature of turbulent transport can be understood by adjusting the coefficients of nonlinear coupling terms. It is identified that the energy inflow due to the nonlinear coupling between turbulence and ZFs or between turbulence and $p_{10}$ pressure perturbation can excite GAMs and simultaneously generate residual ZFs or not. Multiple/single-burst nature in the GAM intermittency originates from qualitatively difference between the two nonlinear coupling terms. Energy backflow due to the nonlinear coupling between turbulence and ion sound parallel velocity cancels the effect of Reynolds stress. When the backflow always overwhelms the inflow due to the Reynolds stress, steady state of turbulence appears. We have also extended the simulations to involve different dissipations such as the collisional damping and the ZP effects. Mixed dissipations can cause different transport behaviours with different time scale. The multiple dissipation mechanisms are found to synergetically couple each other and lead plasmas to complex dynamical transport over long time scale.

### References

1   P. H. Diamond et al., Plasma Phys. Control. Fusion **47**, R35 (2005).

2   A. M. Dimits et al, Phys. Plasmas **7**, 969 (2000).

3   Z. Lin et al., Phys. Rev. Lett. **83**, 3645 (1999).

4   N. Winsor et al., Phys. Fluids **11**, 2448 (1968).

5   K. Hallatschek,et al, Phys. Rev. Lett. **86**, 1223 (2001)

6   B. Scott, Phys. Lett. A **320**, 53 (2003)

7   G. R. McKee, et al., Phys. Plasmas **10**, 1712 (2003)

8   G. D. Conway et al., Plasma Phys. Control. Fusion **47**, 1165 (2005).

9   N. Miyato, Y. Kishimoto, Jiquan Li, Phys. Plasmas **11**, 5557 (2004).

10   K. Miki, Y. Kishimoto, N. Miyato, Jiquan Li, Phys. Rev. Lett. **99**, 145003 (2007).

11   M. A. Malkov, P. H. Diamond, M. N. Rosenbluth, Phys. Plasmas **8**, 5073 (2001).

12   K. Itoh et al., Plasma Phys. Control Fusion **47**, 451 (2005)

13   Jiquan Li and Y. Kishimoto, Phys. Rev. Lett. **89**, 115002 (2002)